5th International Conference
on
Wind Turbine Noise
Denver 28 – 30 August 2013

Acoustic array design for wind turbine noise measurements

Steven Buck University of Colorado Boulder[1]
E-mail: Steven.Buck@colorado.edu
Scott Palo University of Colorado Boulder[1]
Email: Scott.Palo@colorado.edu
Patrick Moriarty National Renewable Energy Laboratory[2]
Email: Patrick.Moriarty@nrel.gov
Jason Roadman National Renewable Energy Laboratory[2]
Email: Jason.Roadman@nrel.gov
Mike Asheim Colorado School of Mines[3]
Email: Mike.Asheim@gmail.com

Summary

An acoustic array for measurement of wind turbine noise has been designed in a collaborative effort by the National Renewable Energy Laboratory and University of Colorado Boulder. The array is built upon 63 electret condenser microphones in a multi-arm logarithmic spiral pattern, a single calibrated B&K precision condenser microphone, in-house designed analog electronics, and an integrated National Instruments data acquisition system. Noise source maps are generated using a delay-and-sum beamforming algorithm with diagonal elimination in the cross-spectral matrix. The uniqueness of this array design over currently available commercial products is its lower frequency range and weather-proof design allowing for long term observational campaigns.

The array has been deployed since late 2012 at the upwind side of the CART-2 research turbine at the National Wind Technology Center. The turbine has a highly instrumented rotor and accompanying meteorological tower enabling noise correlations with both detailed turbine operational characteristics and atmospheric conditions. An active acoustic source has been used to calibrate the array and characterize its performance. Simulated point-source data has been used to compare these results to expected results. The array is shown to have a 3-dB beamwidth of 5.89 meters for a 450 Hz source at the center of the rotor, 56 meters from the center of the array. Turbine noise data has been

[1] University of Colorado, Department of Aerospace Engineering Sciences, 429 UCB, Boulder CO 80303
[2] National Renewable Energy Laboratory, 15013 Denver West Parkway, Denver CO 80401
[3] 1600 Illinois Street, Golden, CO 80401

collected over a range of operational conditions, including wind speeds from 7 to 22 m/s and rotor speeds of up to 42 RPMs (6-second averages). Data from these measurement campaigns have been analyzed at frequencies from 300 Hz to 8 kHz.

1. Introduction

Acoustic arrays are implemented in order to remotely infer the location and strength of sources in an acoustic field. They rely on signals from multiple microphones in order to deduce these spatial characteristics. Arrays have been used both in wind tunnels [1,2] and in the field [3,4] for measurements of noise from locomotives, airfoils, aircraft and aircraft subsystems. However, relatively few studies have been conducted using these devices for measurements of wind turbine noise, particularly on full scale turbines. Oerlemans et al. have conducted such a study in the Netherlands using an array of their design [4,5]. An array has been designed for the purpose of conducting similar research at the National Wind Technology Center (NWTC) in Boulder, Colorado.

This paper discusses the design and use of a multi-arm, logarithmic spiral acoustic array by the National Renewable Energy Laboratory for measurement and characterization of wind turbine generated noise. This design process is a continuation of the elliptical array design work done by Simley [6]. A description of the array system design process is presented, including array shape design, mechanical design, design of electronics and the data acquisition system, and development of post-processing software. System testing and calibration methods are detailed. Finally, results from the initial data acquisition campaign are offered and discussed.

2. Acoustic Array Design

2.1 Design Requirements The National Renewable Energy Laboratory (NREL) requires an acoustic array with several specific characteristics for their experimental purposes. First, in order to facilitate ease of deployment and use, the system has been designed fully weatherproof for sustainable, safe storage in the field. It must be robust to the expected conditions at the NWTC, including snow, rain, high wind and wind-borne debris, and temperatures between about -20°F and 100°F. With the design capable of operating under these conditions, the system can be left entirely assembled in the field for the vast majority of a testing campaign, greatly reducing experimental setup time.

In addition, it was desired that the array be capable of resolving relatively low frequency sources in turbine acoustic output. The low frequency capability of the array can be quantified by its main beamwidth in the plane of the turbine rotor, which scales with wavelength and inversely with array size. In order to reduce the main beamwidth and improve the resolution of the array, the array is significantly larger than commercially available products. For this reason, it has been designed and constructed in-house at the NWTC.

2.2 Array Shape Design The array shape is a zero-redundancy, multi-arm logarithmic spiral layout. The shape was designed in an iterative process based the procedures outlined in Underbrink [7]. The shape is stretched in the streamwise direction to compensate for the viewing angle of about 42° from the turbine hub. The stretching ratio of 2.25 provides improved vertical resolution yet feasible array size. Finally, in practice,

the shape is rotated with its semi-major axis aligned with a point 65% the rotor radius from the hub on the side of the downward passing blade. The stretching and pointing adjustments are in accordance with the methods of Oerlemans et al. [4].

The resulting shape consists of 7 spiral arms each with 9 elements as shown in Figure 1, giving a total of 63 array elements. The performance of the array is characterized using simulation of an ideal, single-frequency point-source in the rotor plane. This provides a visualization of the array point spread function (PSF) as shown in Figure 1, as well as an analytical tool for determining the beamwidth and sidelobe levels and locations. Figure 2 shows the array beamwidth at the hub location as a function of frequency.

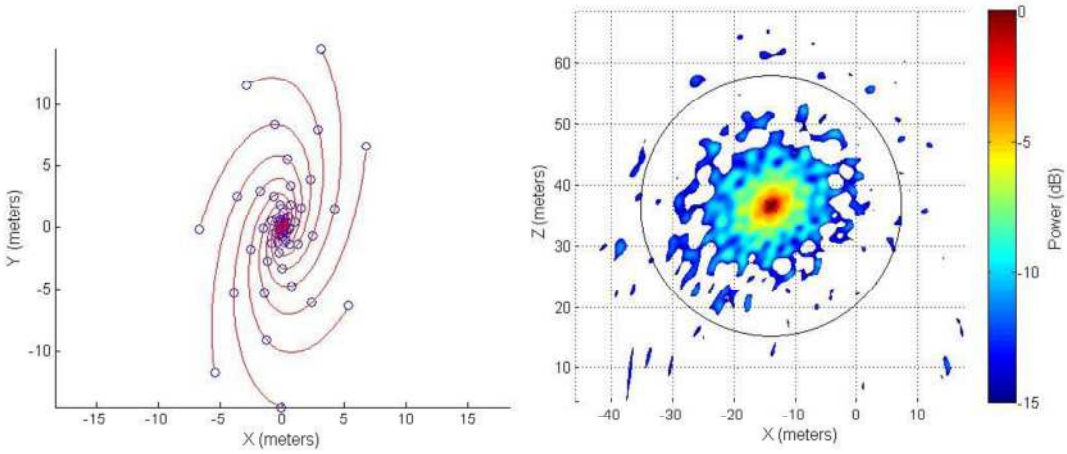

Figure 1: Nominal array shape (left) and point spread function of the design for a 1 kHz point source at the hub of the CART-2 research turbine (right). The circular outline represents the blade tip swept curve of the CART-2 research turbine. Note that X, Y, and Z are in the cross-stream, downstream, and vertically upward directions respectively.

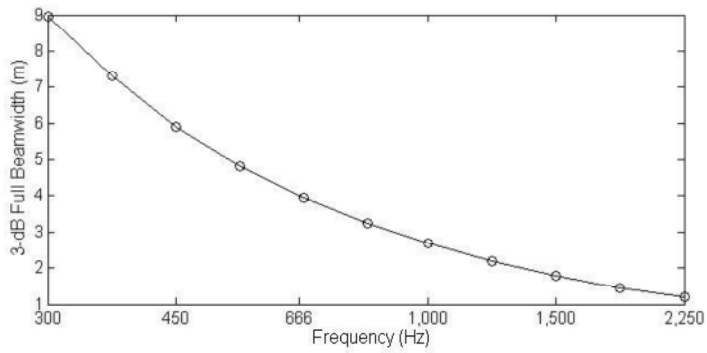

Figure 2: 3-dB full beamwidth of the array versus frequency at a range of 56 meters and elevation angle of 42°.

Figure 2 shows that, as expected, at very low frequencies the array resolution is relatively terse. At 450 Hz, the array has a 3-dB beamwidth of 5.89 m. This resolution does not allow for high precision resolution of noise sources. It does, however, allow for separation of noisy regions, such as nacelle noise from noise near the blade tips.

2.3 Electronics and Data Acquisition Hardware A block diagram of the signal path and data acquisition system is shown in Figure 3. The system utilizes 63 Panasonic WM-64BC electret condenser microphones. Because this particular model was discontinued

after finalization of the design, several channels now utilize PUI Audio POM-2242P-C33-R electret condenser microphones. The two models are electrically and geometrically similar, and the difference in sensitivity of 3-dB is compensated for by calibration.

The microphone signal is amplified in two stages. The first is a differential, BJT based amplifier, which is powered by a DC voltage provided by the second amplification stage. This amplifier outputs a differential signal and is located only several inches of wire from the microphone for improved signal-to-noise ratio. The amplifier is built upon two BC857B PNP transistors. The second stage is a differential to single-ended, non-inverting, op-amp based amplifier with a gain of approximately 220. This stage utilizes two NE5532 op-amp ICs. The two stages are connected by 100 feet of 2-conductor, shielded cable.

The 63 signals are then passed to an integrated National Instruments (NI) data acquisition (DAQ) system. The DAQ is comprised of four, 16-channel NI PXIe-4496 DAQ modules and a PXIe-8108 controller. Each module has a resolution of 24 bits and is capable of simultaneous sampling. A sampling rate of 25 kHz was chosen in order to reduce the size of data files. The resulting Nyquist frequency of 12.5 kHz is sufficient for our interest in low frequency content. The modules' anti-aliasing filters were applied to the incoming signals and are automatically set to the Nyquist rate.

A Brüel & Kjær 4189 precision microphone was positioned in the inner section of the array as a reference signal. It is calibrated with a 94 dB signal at 1 kHz using a Brüel & Kjær 4231 calibration source. The reference signal is then passed to an NI-9233 USB DAQ card, which is also sampled at 25 kHz and anti-alias filtered. The signal is not sampled simultaneously with the array signals, but the lag was shown to be less than 0.06 seconds.

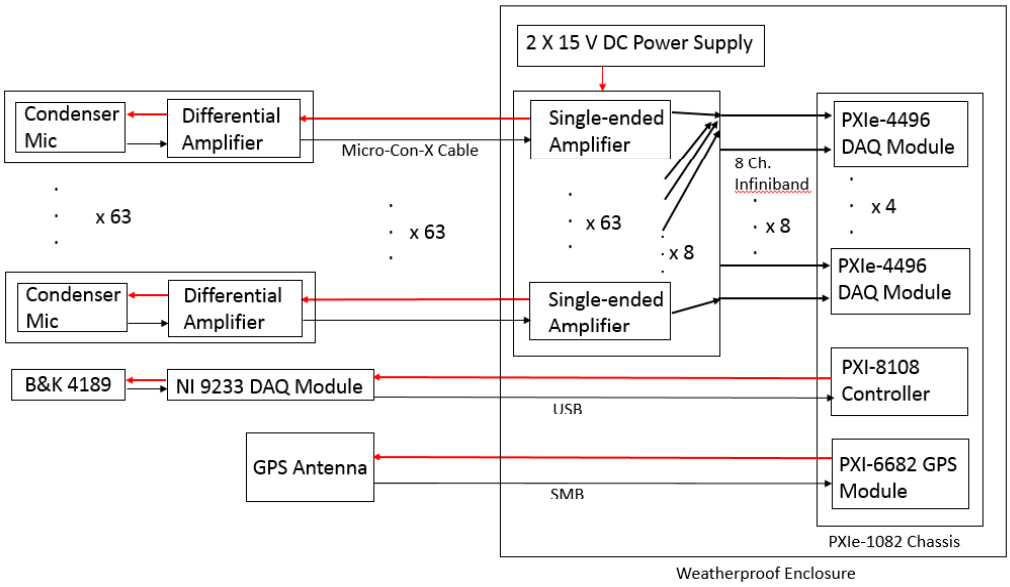

Figure 3: Block diagram of the microphone electrical hardware. Black arrows represent signals/data and red arrows represent power.

Finally, in order to synchronize the array measurements with the instrumentation data from the turbine, an NI PXI-6682 GPS module is used to timestamp all data. This allows for accurate correlation of noise data to atmospheric conditions and turbine operational parameters.

2.4 Field Hardware The array's structural design is based on two segments: the fixed, inner array, which contains between four and five elements of each spiral arm, and the modular outer array. See Figure 4. The inner array is built from 80/20 aluminum extrusions supporting a laser-cut plywood topsheet. The frame is secured by six rebar stakes, each penetrating approximately 18" into the earth.

The modular array elements are each placed on laser-cut, circular plywood mounts of diameter 0.56 m and thickness 13 mm. The mounts are laid flat surrounded by a dirt-mortar mix to minimize edge scattering effects. The dimensions of the modular element mounts are based on recommendations of international standard IEC 61400-11 [8], though the diameter was reduced from the recommended 1 m to 0.56 m for convenience. The recommendation of 1 m diameter is for analysis of frequencies as low as 20 Hz, whereas our analysis does not examine frequencies below 300 Hz. A simple scaling with wavelength implies that 0.56 m will be sufficient for accurate prediction of pressure doubling effects.

Each microphone was placed using an analog survey transit to within 11 cm of the designed location. The microphones coordinates were then measured using an Automated Precision Inc. Tracker3 laser spatial analyzer to an accuracy of 0.05" in each direction, and these coordinates were used for beamforming.

Figure 4: Inner, fixed array structure (left) and outer, modular array element (right).

2.5 Weatherproofing The microphones are mounted on the outside of a waterproof, polycarbonate box approximately 2" on a side that is rated for NEMA-4 water ingress. See Figure 5. The microphone wires are sealed with a waterproof silicone adhesive. The first amplification stages' differential amplifier electronics are housed within each of these small enclosures. Waterproof Micro-Con-X connectors produced by Conxall utilize rubber washers to maintain the waterproof integrity of the box. Custom cabling by the same manufacturer provides the signal path from each microphone to the central data acquisition enclosure. Note that the nominal design and IEC standards call for the use of wind screens, though these were not present during the initial data acquisition campaign

due to time constraints. Hemispherical, 90 mm diameter wind screens will be manufactured from spherical, ACO Pacific outdoor wind screens and included in the final construction.

The data acquisition hardware is enclosed in a large aluminum enclosure. It is approximately 2.5' x 3.5' x 12' in size and is large enough to house the second-stage amplification boards, power supplies, and the National Instruments PXI data acquisition (DAQ) chassis. All hardware inside the chassis is either bolted directly to the backplane or mounted on DIN rails. Micro-Con-X connectors provide the corresponding waterproof signal path into this enclosure from each microphone. The Ethernet and 120VAC power connections use a similar waterproof connector. An electric heater is mounted inside the enclosure to act as a dryer and dehumidifier for condensation during diurnal thermal cycling.

Figure 5: Microphone electronics waterproof enclosure and mount (right) and contained differential amplifier (right).

At the time of this paper's completion, several final modifications must be made to the enclosure's ventilation system to allow maintained deployment at the NWTC. Air circulation must be maintained between the enclosure and the ambient air to provide sufficient cooling for the enclosed electronics. The enclosure is equipped with a fan that draws air into the bottom of the chassis and exhausts at the top through hooded inlet ducts. The edges of these hoods will be waterproofed with aluminium tape extended sufficiently far below the exhaust vents that moisture will not be blown back into the enclosure by strong winds in a rain storm. Additional protection from water ingress through the exhaust hoods will be provided by spring-loaded baffles that seal on weather-stripping when the cooling fan is not operating.

2.5 Data Acquisition and Beamforming Software The data acquisition software has been developed in Labview for seamless integration with the PXI DAQ hardware. The software simultaneously samples the 63 array channels as well as the reference microphone (not simultaneously). The software also enables the PXIe-4496 modules' anti-aliasing filters and reads a timestamp from the PXI-6682 GPS module. All of these features—simultaneous sampling, reference microphone calibration, anti-alias filtering, and GPS timestamping—have been verified on an individual basis.

The beamforming software is written in Matlab and implements a traditional frequency domain delay-and-sum algorithm. Frequency domain implementation improves the speed of the code's execution over the analogous time domain algorithm [6]. The diagonal elements of the cross-spectral matrix are nulled for reduction of the effects of microphone self-noise and electrical noise. Beamforming is typically performed on 6-second sections of data, averaging the effects of between three and four full rotor rotations. The averaging time is reduced or increased based on the consistency of atmospheric conditions.

The software compensates for the effects of sound convection by assuming a constant, identical wind speed and direction between the microphone and scan location, as in [2,3] and based on the geometrical convection analysis of Soderman et al. [9] extended to three dimensions. The merit of this method is tested and discussed in Section 4.2.

3. Field Testing and Calibration

3.1 Active Source Testing The complete array system has been tested using a controlled, active acoustic source in a known location. The source's location is measured by one of two methods: Initially, by using an analog surveying transit, and in later tests with a digital Automated Precision Inc. Tracker3 spatial analyser for improved accuracy. The survey transit provides a knowledge of the source location to within an estimated 71 cm in each direction. The spatial analyser, on the other hand, provides an accuracy of approximately 0.05". The measured location is then compared to the noise maps generated by the beamforming software. The acoustic signal for both testing campaigns is generated using the *sound* function in Matlab and amplified using a Fender, 15-Watt "Rumble 15" bass guitar amplifier. This setup provides both the flexibility and power required for the purposes of these tests.

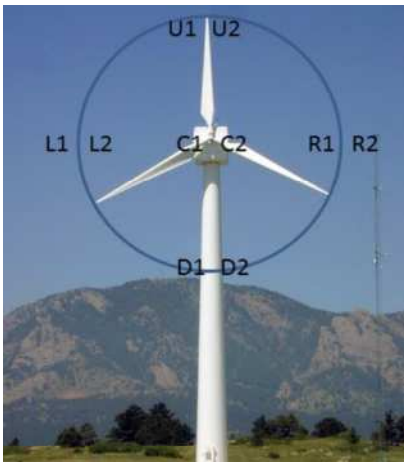

Figure 6: Spatial locations of acoustic source for array system testing.

The initial active source test of the array consists of a matrix of ten spatial locations and three acoustic signals—1.5 kHz and 3.2 kHz pure tones and a broadband signal. The spatial locations are spread throughout the rotor swept region of the Northwind 100A turbine at the NWTC as shown in Figure 6. A hydraulic platform lift was used to raise the source to each of the lettered regions U, D, L, R, and C (up, down, etc.). The source was then moved from the left side of the platform to the right side, denoted by the numbers 1 and 2. The nominal spatial locations are based on analog survey transit measurements, which hold approximately 71 cm of uncertainty in each direction. The relative distance between positions 1 and 2 in each region is also verified by tape measure, which gives higher precision information for comparison to noise map results.

The size of this test matrix lends itself to a statistical description of results. Data was recorded for 90 seconds for each of the three signals for each of the ten locations. The data is broken into six-second sections for beamforming. This gives a total of fifteen, six-second data segments for each frequency and location.

Averaging over all 150 1.5 kHz data sets, a mean position error—the absolute discrepancy between surveyed position and noise map maximum power location—of 77.4 cm exists, and at 3.2 kHz the mean error is 84.8 cm. The standard deviations in noise map maximum power location at 1.5 kHz and 3.2 kHz are 25.1cm and 32.9 cm, respectively. Finally, the mean absolute error in relative distance between positions 1 and 2, averaged over all five regions, was 19.5 cm for the 1.5 kHz source and 12.9 cm for the

3.2 kHz source. The latter result suggests that the magnitude of error in position versus surveyed position is greatly influenced by the uncertainty in surveying data, which was estimated at 71 cm.

Broad band signals were analyzed by the beamforming software over third-octave bands centered about 1.5 kHz and 3.2 kHz. Results hold similar standard deviations between measurements, but the mean absolute error is approximately double. This is likely due to the fact that the same broadband signal was repeatedly used, so the noise would logically result in a consistent error between subsequent measurements.

The above results, along with a qualitative comparison of experimental noise maps to simulation results as in Figure 7, signify that the array and associated software are functioning properly. Errors on the order of several tens of centimeters at a range of 30 meters are deemed acceptable and are attributed to atmospheric conditions during testing. Wind speeds varied between 2 and 6 m/s during these speaker tests and are not taken into account in these noise maps. The effects of atmospheric conditions are discussed further in Section 4.2.

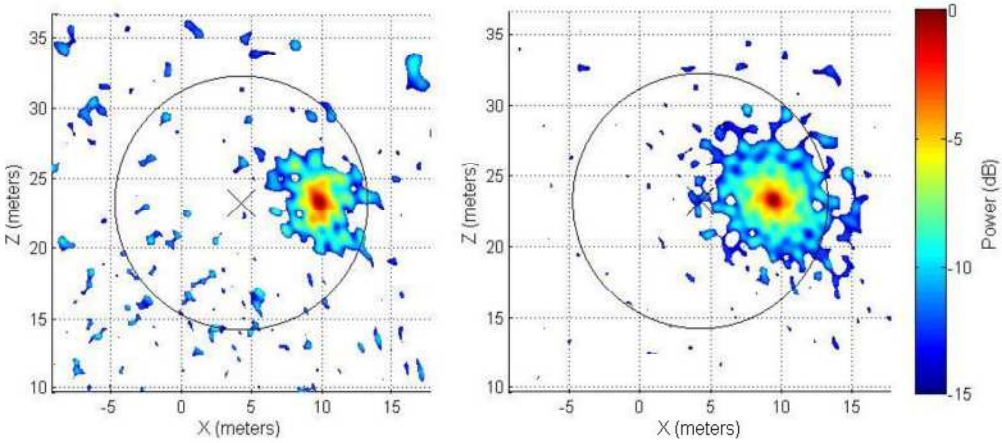

Figure 7: Noise maps generated for experimental data (left) and simulated point-source data (right) for a 1.5 kHz source at location R1.

3.2 Array Calibration Method To compensate for the amplifier gains and microphone sensitivities of each channel, a weighting factor for each signal is included. Dougherty's [10] suggested method involves the derivation of a complex weighting that corrects both amplitude and phase, with phase corrections aiding the imperfect knowledge of microphone location. Our method of microphone location measurement provides knowledge of microphone coordinates to within approximately 0.05" in each direction. This is less than 1/16th of a wavelength for frequencies up to about 16.7 kHz, which is well beyond the range of our analyses. Microphone location errors of this magnitude should cause minimal detriment to beamforming according to the work of Simley [6], and thus our calibration corrects only for amplitude.

An active acoustic source is used for calculation of the weights for each channel. The speaker is placed in the far field of the array and located using the Tracker3 laser spatial

analyzer. A pure tone acoustic signal at 500 Hz is generated and recorded in several 45 second sections of data. The signal is the dominant signal in the acoustic field, with an SNR of approximately 45 dB above adjacent frequencies. Atmospheric attenuation at this frequency is less than 0.5 dB over the range of the array [11] and is neglected. An FFT of the data from each channel is taken in blocks of 1000 samples and averaged over a sufficiently large span of data. The relative magnitudes of each signal are then adjusted for range from the source and normalized to the sensitivity of the reference microphone.

This method also allows for investigation of the weather-readiness of the field equipment. Figure 8 shows the relative sensitivity of each microphone at the deployment of the array in November 2012 and the sensitivities as of May 2013. Microphone boxes were left in the field through the interim period. The comparison illuminates several notable facts. The first is that microphones 1, 20, 21 and 22 had degraded signals, with microphone 20 being nearly out of commission. It was found that the silicone seals was faulty on these microphone boxes, and moisture was present.

Also notable is the significantly *increased* sensitivity of channels 27, 53, and 62 after the winter season. This is not likely attributed to electronics, but potentially due to degradation of the module elements' sand-mortar edge treatment. Edge scattering effects may have caused a standing wave condition on the surface of the circular microphone mounts, affecting the strength of the received signal. This hypothesis must be investigated further, however. Plans are in place to improve the durability of edge treatments.

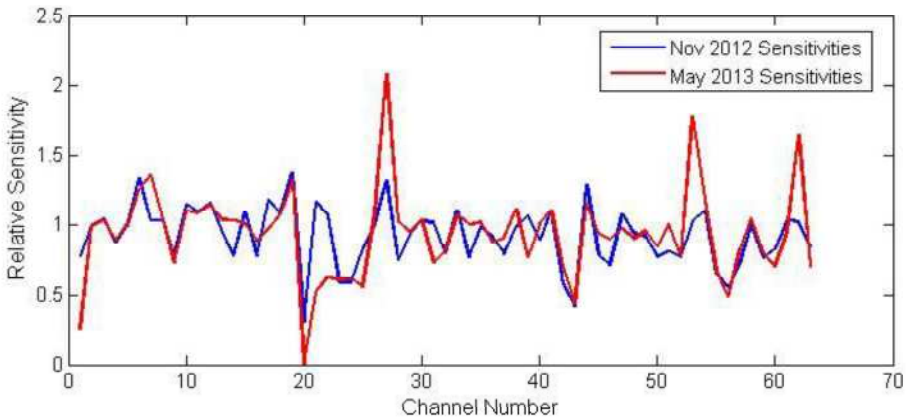

Figure 8: Channel sensitivities relative to channel 2 at deployment of the array versus relative channel sensitivities after the winter season.

4. Turbine Noise Data

4.1 Experimental Setup and Instrumentation The array has been deployed since late 2012 on the westward side—typically upwind--of the CART-2 research turbine at the National Wind Technology Center in Boulder, Colorado. The turbine is a modified, two-

bladed Westinghouse WWG-0600 machine rated at 600 kW. It has a hub height of 36.4 m and a blade-tip radius of 21.3 m. The rotor operates upstream of the tower.

Instrumentation on the turbine and in surrounding area provide turbine operational data and atmospheric condition data sampled at 400 Hz and synchronized with GPS time signals to within a millisecond. Available operational data includes, but is not limited to, nacelle yaw position, rotor azimuth and rotational rate, individual blade pitch angles, and the tilt of the rotor with respect to vertical. Atmospheric conditions available include wind speed and direction at the hub height, top of the rotor, and bottom of the rotor, temperature, and barometric pressure.

The array is located with its center approximately one hub height from the rotor plane. Its semi-major axis aligns with a point 65% the distance from the hub to the blade tip on the downward passing blade under nominal wind conditions. The reference microphone is placed on the inner array platform 32 cm from the nearest array element and 37 cm from the edge of the platform. It is placed in a hemispherical, 16 cm-diameter wind screen.

4.2 Data Acquisition Campaign Since deployment in November 2012, 38 minutes of turbine noise data has been acquired using the array. Data was taken in 45 second segments over the course of several days. 6-second-average wind speeds present in the data span the range from the low-speed cut-in wind speed to 88% the high-speed cut-out wind speed of the turbine—8 m/s and 22 m/s, respectively. Rotor speeds ranged from 15 to 42 RPMs, effectively covering the operational range of the turbine. Data was acquired with the turbine in a feathered position during similar wind conditions for spectral comparisons.

Preliminary analysis of the data reveals several notable characteristics. The first is an unexpected offset, primarily in the vertical direction between the expected location of both mechanical and aerodynamic noise sources, and the locations observed in noise maps. This is discussed further below. The second notable characteristic is the tonal “squeaking” noise caused by the teeter pin of the turbine, which is located at the junction of the two blades. This source has been observed at frequencies between approximately 0.8 and 1.1 kHz. It is generally a very pure tone, which has the benefit of helping to characterize the vertical offset observed.

As discussed in Section 2.5, the beamforming software compensates for sound convection by assuming a constant wind velocity between scan locations and the microphones. Figure 9 shows noise maps for 0.8 kHz—nearly the exact frequency of the teeter noise for this dataset—with and without this compensation. An FFT of the signal shows that the teeter noise has an SNR of about 10 dB above adjacent frequencies. The convection model improves the result by 64 cm in the X-direction and 4.8 meters in the Z-direction. Note that in this particular dataset there was a misalignment of 36° between the rotor-normal and the wind direction, with wind direction rotated counter-clockwise as viewed from above, which explains the correction in the X-direction.

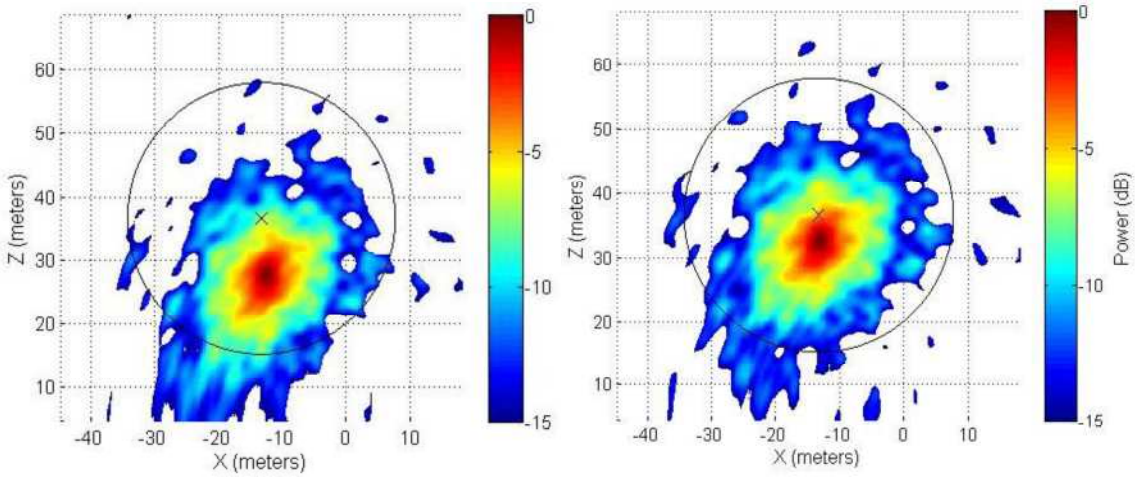

Figure 9: Noise maps for data with 800 Hz teeter noise. The cross hairs represent the nominal location of the teeter pin. The X-direction is horizontal in the plane of the rotor, and the Z-direction is vertical. The average wind speed is 17.21 m/s. The average misalignment angle is 36°, counter-clockwise as viewed from above.

Knowledge of the location of the teeter pin and its relation to the array is precise, and assumed location error cannot account for the offset shown above. It is thusly apparent that the atmospheric model used is not yet sufficient, as an error on the order of four meters is still present after its implementation. The remaining error is attributed to the wind shear profile and turbulence refraction, neither of which are accounted for. This claim is supported by the absence of this error in the results of speaker testing, where there was little wind.

Whereas the teeter noise, when present, dominates the frequency regime just below 1 kHz, trailing edge noise is readily viewed in the regime of 3.2 kHz. Downward passing blade noise is dominant for the majority of data, similar to the results of Oerlemans [2,3], and attributed to convective amplification and source directivity of trailing edge noise. However, in some cases the blade tip noise was dominant on the upward passing blade. Initial analysis, based on five observed cases of this noise map characteristic (6-second averages), points to a potential association with misalignment angles between wind direction and the rotor-normal direction above about 20°, with the wind direction rotated counter-clockwise as viewed from above. Further investigation is required to verify this definitively. Figure 10 shows two noise maps for third-octave bands centered at 3.2 kHz.

Finally, it was noted that the noise source apparent in Figure 10 just below the center of the rotor is present over a frequency range from about 1 kHz to 6 kHz. This is potentially a blade-wake turbulence interaction with the tower or a reflection of blade noise off of the tower. It is not likely due to blade-tower-interaction noise, as this is typically very low frequency and not prevalent in upwind turbines [12]. This phenomenon will be investigated further.

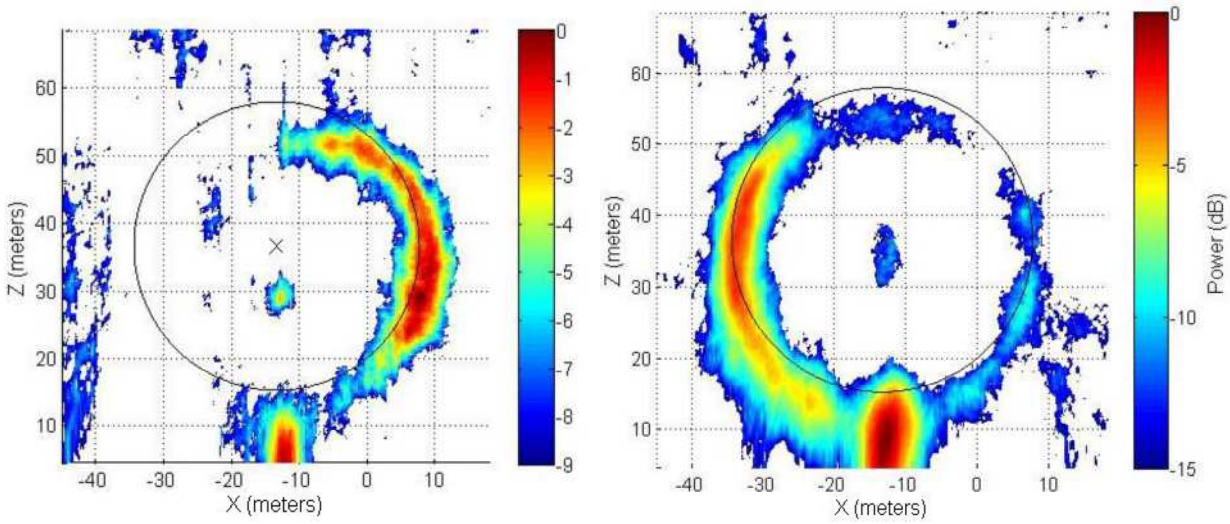

Figure 10: Noise maps for third-octave bands centered at 3.2 kHz. A wind speed of 16.4 m/s and misalignment angle of 2.1° (left) and a wind speed of 16.8 m/s and misalignment angle of 31.3° (right), both counter-clockwise as viewed from above.

5. Conclusions

The array described in this paper is designed for measurement and localization of wind turbine noise. A performance analysis based on active acoustic source testing shows an accuracy of point-source localization on the order of a few tens of centimeters. A non-negligible amount of noise-map variation with atmospheric conditions was observed in both speaker tests and turbine noise data. Implementation of compensation for sound convection helped this matter, removing approximately half of the offset in either direction for the case discussed. Though, a more robust atmospheric model could still significantly improve the system's performance. Initial turbine noise data analyses show that mechanical noise in the nacelle, and particularly teeter-pin squeak, dominates the relatively low frequency output. With increased beamforming frequency, the relative strength of aeroacoustic noise near the blade tip dominates, typically observed on the downward passing blade.

References

1. Bahr, Christopher. *Assessment of Trailing Edge Noise Measurement Techniques.* University of Florida, Department of Mechanical and Aerospace Engineering. 2010.

2. Koop, L., Ehrenfried, K. "Microphone Array Processing for Wind-Tunnel Measurements with Strong Background Noise". *14th AIAA/CEAS Aeroacoustics Conference, AIAA 2008-2907.* Vancouver, British Columbia . May 2005.

3. Zhang, X., Xiao, Y. G., Deng, H. L. "Noise Source Localization Investigation in High Speed Train Based on Microphone Array". Applied Mechanics and Materials, Vol. 103. 2011.

4. Oerlemans, S., Lopez, B. M. "Acoustic Array Measurements on a Full Scale Wind Turbine". *11th AIAA/CEAS Aeroacoustics Conference, AIAA 2005-2963.* Monterey, California. May 2005.

5. Oerlemans, S., Schepers, J. G. "Prediction of wind turbine noise and validation against experiment". International Journal of Aeroacoustics, Vol. 8, No. 6, 2009.

6. Simley, E. *Development of an Acoustic Array for Wind Turbine Aeroacoustic Noise Analysis.* University of Colorado Boulder, Department of Electrical, Computer, and Energy Engineering. 2010.

7. Underbrink, J. R. "*Aeroacoustic Phased Array Testing in Low Speed Wind Tunnels". Aeroacoustic Measurements.* Edited by Thomas J. Mueller. Springer 2002.

8. IEC Norm 61400-11. "Wind turbine generator systems – Acoustic measurement techniques" (2002).

9. Soderman, P. T., Allen, C. S. "*Microphone Measurements IN and Out of Airstream". Aeroacoustic Measurements.* Edited by Thomas J. Mueller. Springer 2002.

10. Dougherty, R. P. "*Beamforming in Acoustic Testing". Aeroacoustic Measurements.* Edited by Thomas J. Mueller. Springer 2002.

11. Blackstock, D. T. *Fundamentals of Physical Acoustics.* John Wiley and Sons, N.Y., 2000.

12. Wagner, S., Bareiß, G., Guidati, G. *Wind Turbine Noise*. Springer 1996.